ChemComm

Accepted Manuscript

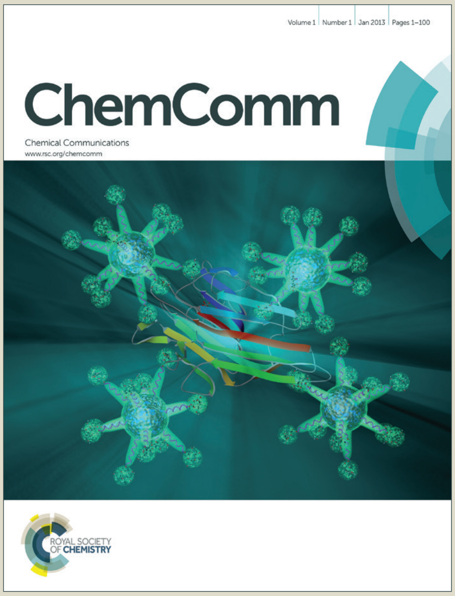

ROYAL SOCIETY OF CHEMISTRY

www.rsc.org/chemcomm

Journal Name RSCPublishing

COMMUNICATION

Cite this: DOI: 10.1039/x0xx00000x

Multiple bands light trapping in ultraviolet, visible, and near infrared regions with TiO_2 based photonic materials†

Zhonghai Zhang,[a,*] and Hongjun Wu [b]

Received 00th January 2012,
Accepted 00th January 2012

DOI: 10.1039/x0xx00000x

www.rsc.org/

The TiO_2 based photonic materials (TiO_2 PMs) with hierarchical top-nanonet/bottom-nanotube structures were fabricated by a facile two-step electrochemical anodization method. The TiO_2 PMs demonstrated multiple bands light trapping activity not only in ultraviolet and visible regions, but also in near infrared region.

Photonic materials (PMs) are periodically structured electromagnetic mediums, with light trapping property by light scatter and diffract, which express great significance in controlling light for display, sensor, telecommunication, and solar energy conversion.[1] Physicists fabricated the PMs by lithographic method, which required complex and expensive instruments and clean-room facilities,[2] while the chemists implemented that in much easier ways by biological templates,[3] polymerized crystalline colloidal arrays,[4] opal hydrogel,[5] and inverse opal hydrogel methods.[6] The most popular chemical method today was the self-assembly of low refractive index PMs, such as silica or polystyrene microspheres,[7] in the form of colloidal crystals to form opals structure, and then replicated the opal template with functional materials, followed by removing the template, then the inverse opal PMs with high reflective index were prepared.[8] However, the inverse opal high reflective index PMs suffer from disadvantages of (1) single band or narrow light trapping region, most of them suppressed in visible light region;[9] (2) existence of cracks,[10] significantly detrimental to the optical properties of the materials.

Titanium dioxide (TiO_2), one of the vital materials for fabrication of solar energy conversion devices, distinguished itself due to its favorable band-edge positions, superior chemical and optical stability, and low lost.[11] The TiO_2 materials with photonic structure would be advantageous for enhancing solar energy conversion efficiency due to its unique light trapping properties, which assured its potential and promising applications in this field. Nowadays, the TiO_2 based PMs have been fabricated by bio- or opal-templates methods,[12] but as well as suffered shortcomings originated from these methods as aforementioned. The preparation of TiO_2 based PMs with multiple bands light trapping property in broad spectrum region, crack-free surface in large scale area by a facile and effective chemical method is still a big challenge.

Very recently, Huang et al reported the fabrication of TiO_2 nanotube based PMs by modulate the multi-layered thickness along the axial direction of the nanotubes, and implemented the enhancement of light trapping in visible region, thus improved the performance of dye sensitized solar cells based on this material.[13] However, to the best of our knowledge, there has no report for TiO_2 based PMs with significantly light trapping properties in near infrared region. In the present study, we report a facile two-step electrochemical anodization approach to prepare a new class of TiO_2 based PMs with broad light trapping activity, which harvest the light not only in ultraviolet and visible regions, but also in near infrared region. The superior optical quality and property guaranteed its potential wide applications in many fields.

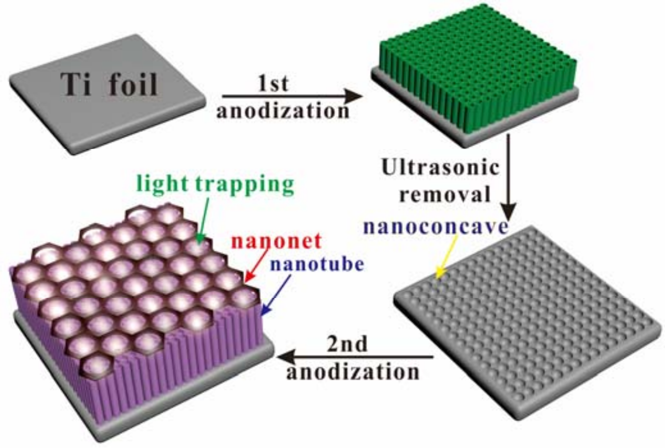

Scheme 1. Two-step electrochemical anodization process for TiO_2 PMs preparation.

The TiO_2 PMs were fabricated in a two-step electrochemical anodization process on the basis of our previous reported methods with novel rationally designed procedure.[14] The detailed preparation processes can be found in Experimental Section (ESI†). Briefly, as shown in **Scheme 1**, the cleaned Ti foil as anode was first anodized in a conventional two-electrode system with Pt mesh as cathode. The electrolyte was ethylene glycol consisted of 0.5 wt% NH_4F and 2 vol% water. The voltage employed in the first-step anodization was 70 V, and then the grown TiO_2 nanotube arrays (TiO_2 NTs) were totally removed in an ultrasonic bath. The high voltage resulted in fast grow rate and high TiO_2 NTs thickness, which was favourable for its removal form the Ti substrate with ultrasonic treatment. The same Ti foil with surface textured nanoconcaves (Fig. S1, ESI†) underwent the second-step anodization with progressive increasing voltages from 10 V to 30 V, thus the hierarchical TiO_2 PMs with top-nanonet/bottom-nanotube structures were fabricated. The successive increasing voltage was vital in the second anodization step for the formation of uniform and periodic nanostructures. The as-anodized TiO_2 PMs were annealed in air at 450 °C for crystallization (XRD pattern in Fig. S2, ESI†). For comparison, one step anodized TiO_2 NTs and two-step anodized TiO_2 NTs at constant voltages in the second step anodization were also prepared.

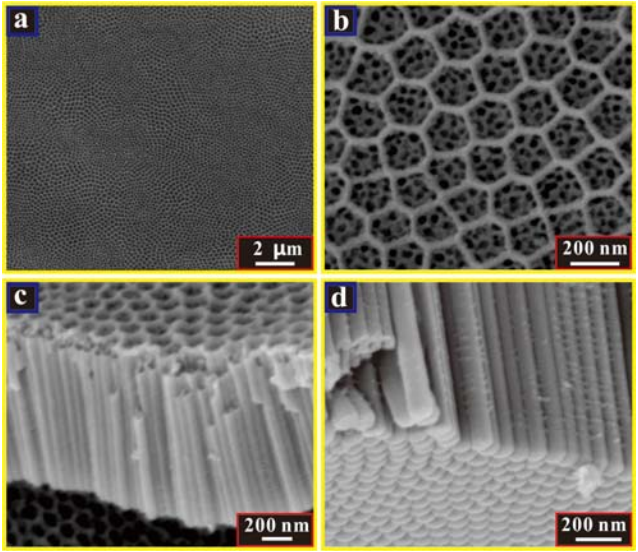

Fig. 1 SEM images of (a) large scale top view of the TiO_2 PMs, (b) high magnification top view of the TiO_2 PMs, (c) cross-sectional view with clear top-net/bottom-tube structures, and (d) bottom surface with close packed nanotubes.

The morphology of the TiO_2 PMs was determined by filed-emission scanning electron microscope (FESEM, FEI Quanta 600). **Fig. 1a** shows the large scale SEM image of the TiO_2 PMs, as expected, a uniform and clean top surface is observed, no any cracks and debris can be found. The high magnification SEM image is presented in **Fig. 1b**, which indicates clear hexagon nanonets on the top, and vertical nanotubes underneath. The top nanonet shows an average diameter of 160 nm, and frame thickness of ~50 nm. The diameter of nanonet is equal to the diameter of nanoconcaves on the textured Ti surface, and the network frame thickness is similar with the ridge thickness on nanoconcaves (Fig. S1, ESI†), which implies that the top-nanonet structure is formed with textured nanoconcave as template. The high magnification cross-sectional view SEM image (**Fig. 1c**) confirms the hierarchical top-net/bottom-tube nanostructure with the top layer thickness being ~50 nm and the bottom-tube diameter in the range of 60-70 nm. The bottom of nanotubes is closed and hexagonally packed as shown in **Fig. 1d**, which is helpful for the formation of nanoconcaves underneath the nanotubes.

The one-step anodized TiO_2 NTs were also prepared, which show severe cracking and fragile bundling debris on the surface (Fig. S3, ESI†). The TiO_2 NTs, prepared by two-step anodization method with constant anodized voltages (30 V and 60 V) in the second-step anodization process, fail to show uniform and periodic nanonet structures. The 30 V anodized sample presents random nanoring structure on the top layer (Fig. S4, ESI†), and the 60 V anodized sample presents uniform nanopore structures (Fig. S5, ESI†), however, the pore size is too small to interact with long wavelength light.

The crystalline structure of TiO_2 PMs was analyzed by X-ray diffraction (XRD, Bruker D8 Discover diffractometer, using Cu Kα radiation, $\lambda = 1.540598$ Å). The strong XRD diffraction peak at 25.3° indicates highly crystallized and dominant anatase phase with preferential orientation of (101) (TiO_2: JCPDS No. 21-1272, Ti: JCPDS No. 44-1294) (Fig. S2, ESI†).The chemical components and surface chemical state of TiO_2 PMs were characterized by photoelectron Spectroscopy (XPS) with an Axis Ultra instrument (Kratos Analytical) under ultrahigh vacuum ($<10^{-8}$ torr) (Fig. S6, ESI†). The survey spectra of the TiO_2 PMs confirm its pure TiO_2 constituent. The high resolution spectra of Ti 2p present dominant peaks centered at 458.6 eV (Ti $2p_{3/2}$) and 464.3 eV (Ti $2p_{1/2}$), which associate with Ti ions with a formal valence of four (Ti^{4+}).[15] The core-level XPS of O 1s show a two-band structure, with dominant peak at 529.8 eV for the oxygen in TiO_2 lattice, and an additional peak at 532.0 eV for the oxygen in hydroxyl.[16]

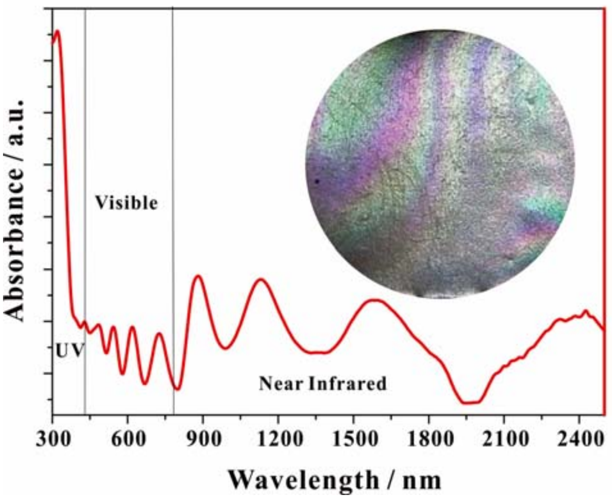

Fig. 2 UV-vis-NIR diffuse reflectance absorption spectra of TiO_2 PMs, the inset presents a digital photo of the TiO_2 PMs.

The diffuse reflectance UV-vis-NIR (ultraviolet-visible-near infrared) absorption spectra of TiO_2 PMs were recorded on spectrophotometer (Shimadazu, UV 3600) with fine $BaSO_4$ powder as reference. As presented in **Fig. 2**, multiple absorption peaks around 320, 428, 482, 542, 620, 725, 879, 1128, 1585, and 2430 nm were clearly observed in UV, visible, and near infrared light regions due to its featured photonic structure. The strong UV absorption below 380 nm can be ascribed to its excitation through band gap. The absorption reached maximum at 320 nm, which can be explained by strong light diffraction induced by the well matching of half wavelength with the top-nanonet's diameter (160 nm). The other moderate absorption peaks in visible and infrared regions can be ascribed to two concurrent processes: first, the light possesses slower transport velocity in high refractive index medium than in air, which results in higher reflectivity, and prolongs the interact time between light and the surrounding sample, enhancing the efficiency of scattering processes, leading to further improvement of light trapping.[1a,17] Second, the unique hierarchical top-nanonet/bottom-nanotube structure acted like a Fabry-Pérot resonator, induced strong finite-size effects, and presented characteristic oscillations and resonances.[18] The top inset in **Fig. 2** shows an actual photo of a TiO_2 PMs, in which presents a visual colour patterns on the surface, provides a macroscopic evidence of the formation of a unique photonic structure. It is worth mentioning that the one-step TiO_2 NTs sample did not show any photonic property (Fig. S7, ESI†), due to its rough and dis-uniform surface. The two-step samples prepared with constant voltages presented strong peak in UV region and broad absorption in visible region, but failed to show multiple peaks characterization (Fig. S8, and Fig. S9, ESI†).

The formation of TiO_2 PMs in anodization processes is an outcome of competition between electric field driven oxidation of metal to form oxide and chemical and field-assisted dissolution of the metal oxide layer.[19] The overall reactions of the two processes can be presented as:

$$H_2O \rightarrow OH^- + H^+ \qquad (1)$$

$$OH^- \rightarrow O_2^- + H^+ \qquad (2)$$

$$Ti + 2O_2^- \rightarrow TiO_2 + 4e^- \qquad (3)$$

$$TiO_2 + 6F^- + H^+ \rightarrow TiF_6^{2-} + 2H_2O \qquad (4)$$

The dissolution in the form of $[TiF_6]^{2-}$ is highly affected by the applied electric field. In the second anodization step, electric field existed in the bottom of concave possessed higher intensity than that at the top surface, which induced the faster dissolution rate in the middle of the nanoconcave, thus preferred for the formation of TiO_2 NTs into depth, but remained the edge of concave to form network structure. The SEM image of TiO_2 PMs was anodized with short time (Fig. S10, ESI†) helps to prove the proposed mechanism. In addition, in this study, the step-wise increasing voltages compensated the loss of electric field intensity due to the formation of thick oxide layer. Compared to constant voltage, the increased voltages would improve the periodicity and uniformity of the top layer, which are the critical factors for formation of TiO_2 PMs.

In summary, we successfully fabricated TiO_2 PMs by a facile two-step electrochemical anodization method. The prepared TiO_2 PMs not only showed strong light trapping activity in UV and visible region, but also possessed infrared light harvesting activity, implemented multiple bands light trapping activity in broad spectrum.

Z.Z thanks to the support from “Yingcai” program of ECNU, and Shanghai Pujiang Program (14PJ1403400), and H.W thanks to the support from New Century Excellent Talent Project of the Department of Education (No. 1253-NCET004), Heilongjiang Province, P. R. China.

Notes and references

[a]*Department of Chemistry, East China Normal University, 500 Dongchuan Road, Shanghai 200241, China.*
Address correspondence to zhzhang@chem.ecnu.edu.cn
[b]*Provincial Key Laboratory of Oil & Gas Chemical Technology, College of Chemistry & Chemical Engineering, Northeast Petroleum University, Daqing 163318, China.*

† Electronic Supplementary Information (ESI) available: Experimental details, XRD, XPS, additional SEM images and DRS spectra. See DOI: 10.1039/c000000x/

1 (a) G. von Freymann, V. Kitaev, B. V. Lotsch and G. A. Ozin, *Chem. Soc. Rev.*, 2013, **42**, 2528; (b) I. B. Burgess, L. Mishchenko, B. D. Hatton, M. Kolle, M. Lončar and J. Aizenberg, *J. Am. Chem. Soc.*, 2011, **133**, 12430; (c) W. Hong, Y. Chen, X. Feng, Y. Yan, X. Hu, B. Zhao, F. Zhang, D. Zhang, Z. Xu and Y. Lai, Chem. Commun., 2013, 49, 8229; (d) M. E. Calvo, S. Colodrero, N. Hidalgo, G. Lozano, C. López- López, O, Sánchez-Sobrado and H. Míguez, *Energy Environ. Sci.*, 2011, **4**, 4800; (e) S. Foster and S. John, *Energy Environ. Sci.*, 2013, **6**, 2972.

2 (a) S. Yamada, B. S. Song, T. Asano, S. Noda, *Appl. Phys. Lett.*, 2011, **99**, 201102; (b) M. F. Yanik and S. Fan, *Phys. Rev. Lett.*, 2004, **92**, 083901.

3 (a) Q. Yang, S. Zhu, W. Peng, C. Yin, W. Wang, J. Gu, W. Zhang, J. Ma, T. Deng, C. Feng and D. Zhang, *ACS Nano*, 2013, **7**, 4911; (b) C. Mille, E. C. Tyrode and R. W. Corkery, *Chem. Commun.*, 2011, **47**, 9873.

4 (a) J. T. Zhang, L. Wang, X. Chao, S. S. Velankar and S. A. Asher, *J. Mater. Chem. C*, 2013, **1**, 6099; (b) N. Sai, B. Ning, G. Huang, Y. Wu, Z. Zhou, Y. Peng, J. Bai, G. Yu and Z. Gao, *Analyst*, 2013, **138**, 2720.

5 (a) X. Hong, Y. Peng, J. Bai, B. Ning, Y. Liu, Z. Zhou and Z. Gao, *Small*, 2014, **10**, 1308; (b) C. G. Schäfer, M. Gallei, J. T. Zahn, J. Engelhardt, G. P. Hellmann and M. Rehahn, *Chem. Mater.*, 2013, **25**, 2309.

6 (a) B. Mandlmeier, J. M. Szeifert, D. Fattakhova-Rohlfing, H. Amenitsch and T. Bein, *J. Am. Chem. Soc.*, 2011, **133**, 17274; (b) S. Kado, H. Otani, Y. Nakahara and K. Kimura, *Chem. Commun.*, 2013, **49**, 886; (c) Y. J. Lee and P. V. Braun, *Adv. Mater.*, 2003, **15**, 563.

7 (a) J. T. Zhang, X. Chao and S. A. Asher, *J. Am. Chem. Soc.*, 2013, **135**, 11397; (b) A. Blanco, E. Chomski, S. Grabtchak, M. Ibisate, S. John, S. W. Leonard, C. Lopez, F. Meseguer, H. Miguez, J. P. Mondia, G. A. Ozin, O. Toader and H. M. van Driel, *Nature*, 2000, **405**, 437.

8 (a) Q. Yang, M. Li, J. Liu, W. Shen, C. Ye, X. Shi, L. Jiang and Y. Song, *J. Mater. Chem. A*, 2013, **1**, 541; (b) F. Sordello, C. Duca, V. Maurino and C. Minero, *Chem. Commun.*, 2011, **47**, 6147.

9 J. Wang, Y. Hu, R. Deng, R. Liang, W. Li, S. Liu and J. Zhu, *Langmuir*, 2013, **29**, 8825.

10 Z. Zhang, W. Shen, C. Ye, Y. Luo, S. Li, M. Li, C. Xu and Y. Song, *J. Mater. Chem.*, 2012, **22**, 5300.

11 (a) J. Zhu, J. Wang, F. Lv, S. Xiao, C. Nuckolls and H. Li, *J. Am. Chem. Soc.*, 2013, **135**, 4719; (b) Z. Zhang and P. Wang, *Energy Environ. Sci.*, 2012, **5**, 6506.

12 (a) T. Ding, Y. Long, K. Zhong, K. Song, G. Yang and C. H. Tung, *J. Mater. Chem. C*, 2014, **2**, 4100; (b) X. Zheng, D. Li, X. Li, L. Yu, P. Wang, X. Zhang, J. Fang, Y. Shao and Y. Zheng, *Phys. Chem. Chem. Phys.*, 2014, **16**, 15299.

13 (a) C. T. Yip, H. Huang, L. Zhou, K. Xie, Y. Wang, T. Feng, J. Li and W. Y. Tam, *Adv. Mater.*, 2011, **23**, 5624; (b) M. Guo, Z. Yong, K. Xie, J. Lin, Y. Wang and H. Huang, *ACS Appl. Mater. Interfaces*, 2013, **5**, 13022.

14 (a) Z. Zhang, L. Zhang, M. N. Hedhili, H. Zhang and P. Wang, *Nano. Lett.*, 2013, **13**, 14; (b) Z. Zhang, M. N. Hedhili, H. Zhu and P. Wang, *Phys. Chem. Chem. Phys.*, 2013, **15**, 15637.

15 (a) B. Liu and H. C. Zeng, *Chem. Mater.*, 2008, **20**, 2711; (b) Z. Zhang, X. Yang, M. N. Hedhili, E. Ahmed, L, Shi and P. Wang, *ACS Appl. Mater. Interface*, 2014, **6**, 691.

16 J. C. Yu, L. Zhang, Z. Zheng and J. Zhao, *Chem. Mater.*, 2003, **15**, 2280.

17 S. A. Rinne, F. Garcia-Santamaria and P. V. Braun, *Nat. Photonics*, 2008, **2**. 52.

18 N. Gaber, M. Malak, F. Marty, D. E. Angelescu, E. Richalot and T. Bourouina, *Lab Chip*, 2014, **14**, 2259.

19 (a) H. Mirabolghasemi, N. Liu, K. Lee and P. Schmuki, *Chem. Commun.*, 2013, **49**, 2067; (b) M. Ye, X. Xin, C. Lin and Z. Lin, *Nano. Lett.*, 2011, **11**, 3214; (c) F. Wang, Y. Liu, W. Dong, M. Shen and Z. Kang, *J. Phys. Chem. C*, 2011, **115**, 14635.